Molecular mechanisms of kinetochore capture by spindle microtubules

Kozo Tanaka[1], Naomi Mukae[1], Hilary Dewar[1], Mark van Breugel[2], Euan K. James[1], Alan R. Prescott[1], Claude Antony[3] & Tomoyuki U. Tanaka[1]

[1]*School of Life Sciences, University of Dundee, Wellcome Trust Biocentre, Dundee DD1 5EH, UK*
[2]*Max Planck Institute of Molecular Cell Biology and Genetics, 01307 Dresden, Germany*
[3]*European Molecular Biology Laboratory, D-69117 Heidelberg, Germany*

For high-fidelity chromosome segregation, kinetochores must be properly captured by spindle microtubules, but the mechanisms underlying initial kinetochore capture have remained elusive. Here we visualized individual kinetochore–microtubule interactions in *Saccharomyces cerevisiae* by regulating the activity of a centromere. Kinetochores are captured by the side of microtubules extending from spindle poles, and are subsequently transported poleward along them. The microtubule extension from spindle poles requires microtubule plus-end-tracking proteins and the Ran GDP/GTP exchange factor. Distinct kinetochore components are used for kinetochore capture by microtubules and for ensuring subsequent sister kinetochore bi-orientation on the spindle. Kar3, a kinesin-14 family member, is one of the regulators that promote transport of captured kinetochores along microtubules. During such transport, kinetochores ensure that they do not slide off their associated microtubules by facilitating the conversion of microtubule dynamics from shrinkage to growth at the plus ends. This conversion is promoted by the transport of Stu2 from the captured kinetochores to the plus ends of microtubules.

Sister chromatid segregation to opposite poles of the cell during mitosis is crucial for maintenance of genetic integrity in eukaryotic cells. For high-fidelity chromosome segregation, kinetochores must be properly captured by spindle microtubules[1]. In vertebrate cells, after nuclear envelope breakdown, kinetochores are initially captured by the lattice (the lateral surface, rather than the tip) of a single microtubule extending from a spindle pole[2–4]. Kinetochores are then transported poleward along the surface of a microtubule that terminates distal to the kinetochores. During their poleward travel, kinetochores interact with more microtubules, the plus ends of which subsequently become embedded into the kinetochore plates (end-on attachment). Eventually, each sister kinetochore attaches to the plus ends of microtubules from opposite spindle poles. In this way, sister kinetochores bi-orient on the mitotic spindle before anaphase onset. Because kinetochore capture and transport have only been visualized in very few cell types and on limited occasions, mechanisms of kinetochore capture by microtubules have remained elusive.

Recently, centromere movements were visualized in the budding yeast *S. cerevisiae* by marking individual centromeres with green fluorescent protein (GFP)[5–8]. When sister kinetochores bi-orient, the centromere GFP signals split on the pre-anaphase spindle while sister chromatids are still being held together by cohesion along their arms. However, it is poorly understood how kinetochores interact with microtubules before they bi-orient on the spindle. In *S. cerevisiae*, centromeres are tethered by microtubules to spindle pole bodies (SPBs) during most of the cell cycle[9,10]. Nonetheless, centromeres are released from, and recaptured by, microtubules during a brief period in S phase, probably due to kinetochore disassembly and reassembly upon centromere DNA replication[10,11]. Kinetochore capture by microtubules can therefore be studied in budding yeast. However, because all kinetochores are captured by microtubules during a short time period and within a small space around SPBs, it has been difficult to resolve individual kinetochore capture events using light microscopy.

Visualizing kinetochore capture and transport

To visualize individual kinetochore–microtubule interactions in *S. cerevisiae*, we devised the following system (Fig. 1a). We replaced *CEN3* on chromosome III with *CEN3* under control of the *GAL1-10* promoter[12], to conditionally inactivate and activate the centromere by turning on and off transcription from the *GAL-10* promoter in the presence of galactose and glucose, respectively. In addition, to enable detection of *CEN3* in live cells, we marked the *CEN3* sequence by the adjacent insertion of a *tet* operator array that is bound by Tet repressors fused with GFP[13]. Furthermore, microtubules were visualized by expressing α-tubulin (*TUB1*) fused with yellow fluorescent protein (YFP). To conditionally arrest cells in metaphase, the *CDC20* gene, which is required for sister chromatid separation and for anaphase onset[14], was placed under control of the *MET3* promoter, which can be turned off in the presence of methionine. To observe individual kinetochore–microtubule interactions, we wanted to detect the GFP-marked *CEN3* distant from the spindle and from all other centromeres locating on the spindle. To this end, we inactivated the *CEN3* upon the release of cells from α-factor arrest. Simultaneously, we also depleted Cdc20 protein levels to arrest cells in metaphase. Once cells were arrested in metaphase, we reactivated *CEN3* by turning off the adjacent *GAL1-10* promoter while cells were still in metaphase, and followed the behaviour of *CEN3*.

Two hours after release from α-factor arrest, cells were arrested in metaphase and *CEN3* was distant from the spindle in 60–70% of cells. After *CEN3* reactivation, the GFP-marked centromere interacted with microtubules extending from a spindle pole, and moved poleward along the microtubules (Fig. 1b and Supplementary Video S1).

To study kinetochore capture and transport in detail, we wanted to observe longer microtubules because their dynamics can be characterized more precisely. We achieved this by arresting cells in metaphase for longer periods, which led to elongation of the nucleus between buds and mother cell bodies. This elongation was probably due to earlier back-and-forth motions of the spindle between the two cell bodies, and was not due to cells leaking into anaphase, because the spindle length stayed short. When *CEN3* and the spindle were located on opposite sides of such elongated nuclei, microtubules extended for a longer distance from a spindle pole, and captured *CEN3* after *CEN3* reactivation (see Fig. 1c, Supplementary Video S2 and Supplementary Fig. S1). *CEN3* seemed to be captured laterally by microtubules and transported poleward along them. Sometimes *CEN3* motion halted or occurred

anti-poleward for a short period, but eventually poleward motion predominated (for example, Fig. 3a, bottom). Shortly after *CEN3* reached a spindle pole (<5 min), the majority of its GFP signal split on the spindle, indicating that sister *CEN3*s had bi-oriented on the spindle[5–8]. During transport along microtubules, *CEN3* sometimes transiently detached from the microtubules, or changed its associated microtubules to different ones extending from either the same or the opposite pole (Supplementary Fig. S2, Supplementary Video S3). (See Supplementary Note 1.)

To rule out the possibility that kinetochores are pulled by end-on attached microtubules that might have overlapped longer microtubules, we first visualized Bik1 and Bim1, both of which localized to the plus ends of microtubules extending from spindle poles. As *CEN3* moved poleward along microtubules, Bik1 and Bim1 signals always localized distal to *CEN3*, but not at *CEN3* (Supplementary Fig. S3 and Supplementary Note 2). Second, in many cases, the intensity of YFP–Tub1 signals was almost constant along the length of the *CEN3*-associated microtubule, from the spindle pole to the plus end (Supplementary Fig. S4a and Supplementary Video S4). These observations confirm that *CEN3* is indeed captured and transported along the sides of microtubules.

To address whether *CEN3* is captured by a single microtubule, we compared YFP–Tub1 signals from *CEN3*-associated microtubules and from the thinnest cytoplasmic microtubules (Supplementary Fig. S4b), which constitute the majority of cytoplasmic microtubules and are thought to be singular[15,16]. For the majority of *CEN3*-associated microtubules, the intensity of YFP–Tub1 signals was similar to that of the thinnest cytoplasmic microtubules. Thus, many kinetochore-associated microtubules are probably singular, although sometimes other microtubules grew from a spindle pole, overlapping the microtubule that had extended earlier. (See Supplementary Note 3.)

We then addressed whether *CEN3* facilitates nuclear microtubule extension from spindle poles in its direction before capture, or whether microtubule extension occurs in random directions within the nucleus. To distinguish nuclear microtubules from cytoplasmic microtubules, we labelled the nuclear periphery and used a marker for cytoplasmic microtubules (Supplementary Fig. S5). We compared the number of nuclear microtubules that extended towards *CEN3* and away from it (Supplementary Fig. S6). The direction of nuclear microtubules, initially extending from spindle poles, was largely unaffected by the position of free kinetochores that had not yet been captured by microtubules. (See Supplementary Note 4.)

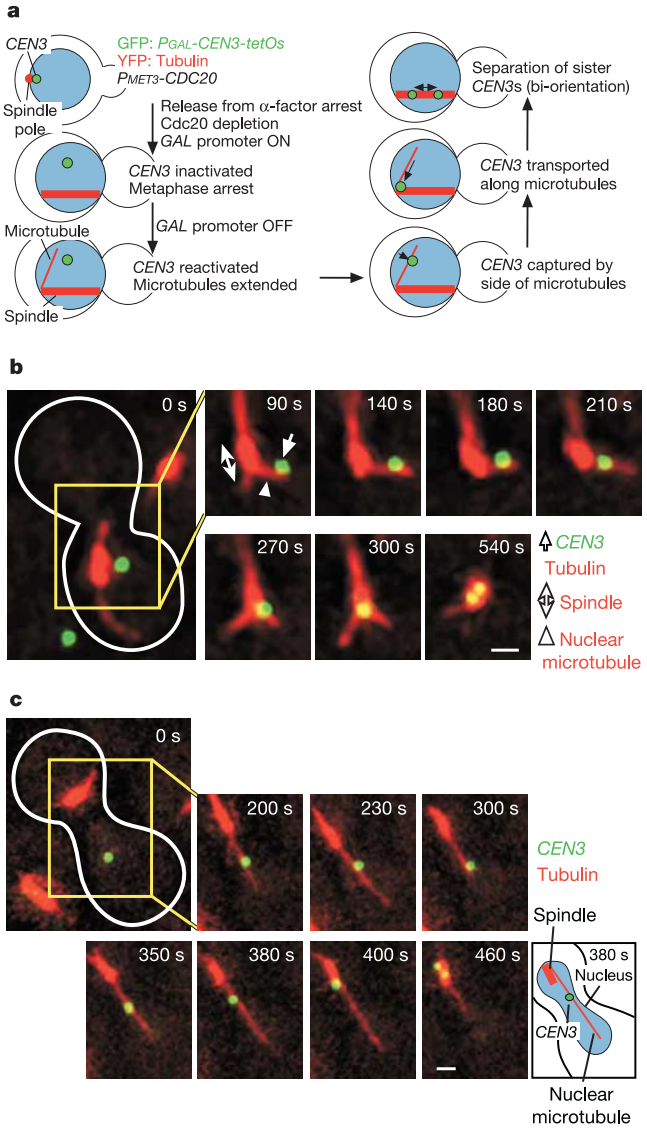

Figure 1 Visualizing kinetochore capture and transport along microtubules. **a**, Experimental system and diagrams showing kinetochore capture. **b**, **c**, Time-lapse images. *P_{MET3}-CDC20 P_{GAL}-CEN3-tetOs TetR–GFP YFP–TUB1* cells (T3531) were treated with α-factor in methionine drop-out medium with raffinose for 2.5 h, and then released to YP medium containing galactose, raffinose and 2 mM methionine. After 2 h (**b**) or 3 h (**c**), cells were suspended in synthetic complete medium containing glucose and methionine. Images were collected every 10 s using separate channels for GFP (*CEN3*; green) and YFP (tubulin; red). Zero time is set arbitrarily for the first panel, in which the cell shape is outlined in white. Scale bar, 1 μm. See Supplementary Videos S1 and S2.

Nuclear microtubule extension and kinetochore capture

We studied the roles of candidate regulators in generating nuclear microtubules from spindle poles and in kinetochore capture by these microtubules. In *S. cerevisiae*, kinetochores contain a number of protein complexes[17]: the CBF3 complex (containing Ndc10) directly binds the centromere DNA; the Dam1 complex (containing Spc34 and Ask1) is thought to provide a direct interface for microtubule attachments to kinetochores in metaphase; the Ndc80 (containing Spc24 and Spc25), Mtw1 (containing Dsn1) and Ctf19 (containing Okp1) complexes are probable components bridging a gap between the CBF3 complex with centromeres and the Dam1 complex with microtubules; and finally, the Ipl1-Sli15 complex (orthologue of the metazoan Aurora B-INCENP complex) ensures sister kinetochore bi-orientation[10,18]. Kinetochore–microtubule interactions might also be regulated by the microtubule plus-end tracking proteins (+TIPs) Bim1, Bik1, Stu1 and Stu2 (orthologues of vertebrate EB1, CLIP170, CLASP and XMAP215/ch-TOG, respectively)[19], and by the small GTPase Ran and its regulators Prp20 (also called Mtr1) and Rna1, which operate as a nuclear Ran GDP/GTP exchange factor (GEF) and a cytoplasmic Ran GTPase-activating protein (GAP), respectively[20]. Although Ran GEF and Ran GAP regulate nuclear import and export in yeast and metazoan cells, they also regulate spindle formation and kinetochore function after nuclear envelope breakdown (open mitosis) in metazoan cells[21,22]. It is not clear whether this is the case in budding yeast, in which the nuclear envelope remains intact throughout the cell cycle (closed mitosis)[9].

We first determined which factors facilitate nuclear microtubule extension from spindle poles. We counted the number of nuclear microtubules in elongated nuclei of mutants of the above regulators. *ndc10-1*, *spc24-1*, *spc25-1*, *dsn1-7*, *mtw1-11*, *okp1-5*, *spc34-3*, *ask1-3*, *dam1-1*, *ipl1-321*, *sli15-3* and *rna1-1* mutants showed similar numbers of nuclear microtubules compared to 'wild-type' cells (cells without mutation; Fig. 2a and data not shown). In contrast, the number of nuclear microtubules was significantly reduced in *prp20-1*, *mtr1-1*, *stu2-10*, *bim1Δ* and *bik1Δ* mutants (Fig. 2a, b and

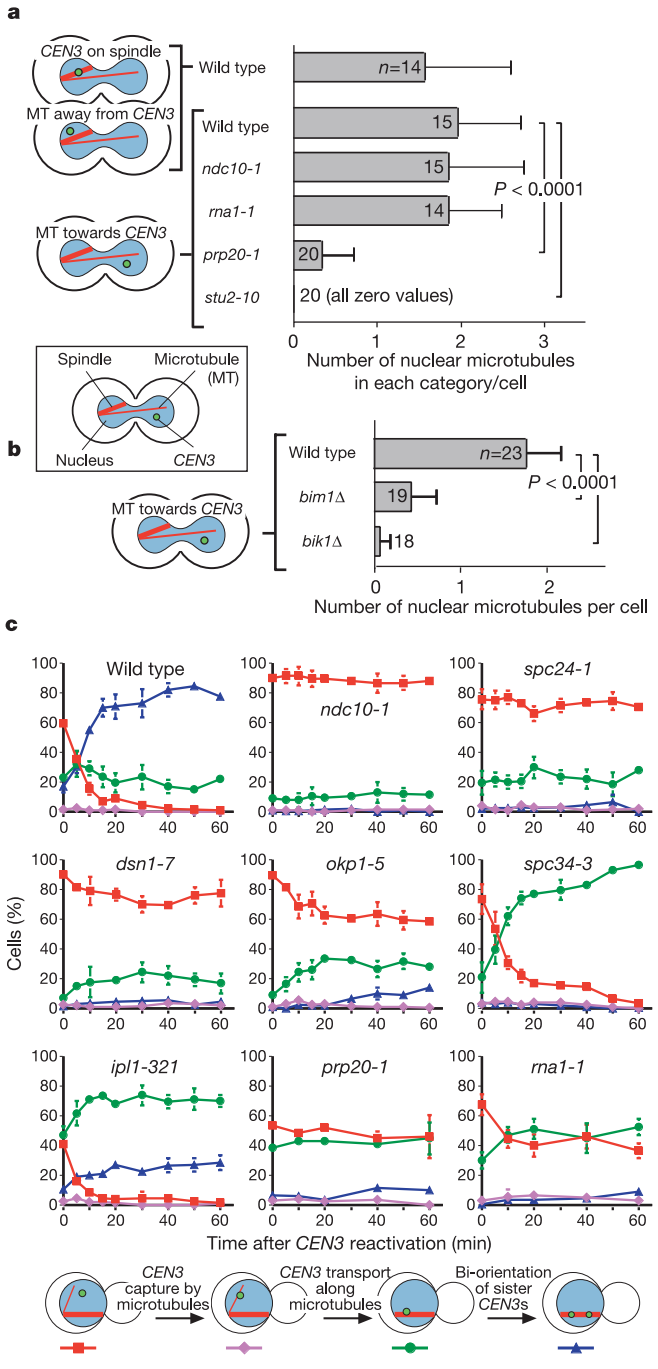

Figure 2 Mechanisms for nuclear microtubule extension and for kinetochore capture. **a**, **b**, Number of nuclear microtubules. *P_{MET3}-CDC20 P_{GAL}-CEN3-tetOs TetR–GFP YFP–TUB1 YFP–NIC96 KIP2–4GFP* (T3270 or 'wild type') cells, and cells with the same genotype but including different mutations (*ndc10-1*, *rna1-1*, *prp20-1*, *stu2-10*, *bim1Δ* or *bik1Δ*) were treated as in Fig. 1c (**b**), or as in Fig. 1c but with cultures shifted to 35 °C (restrictive temperature) 30 min before transfer to glucose-containing medium (**a**). Time-lapse images were collected at 35 °C (**a**) or at 23 °C (**b**) every 10 s for 30 min. Only microtubules that extended from the spindle to the other side (towards the right in diagrams) of elongated nuclei were counted, after cells were classified by *CEN3* location at the beginning of time-lapse. *n* represents the number of observed cells. **c**, Time course for *CEN3* capture. T3531 'wild-type' cells (see Fig. 1 legend) and strains with the same genotype but including different mutations (*ndc10-1*, *spc24-1*, *dsn1-7*, *okp1-5*, *spc34-3*, *ipl1-321*, *prp20-1*, *rna1-1*) were treated as in **a** and fixed at the indicated time points (see Supplementary Note 17e). Coloured lines show the percentage of cells in which *CEN3* has not yet been captured by microtubules (red), in which *CEN3* is on the microtubule extending from a spindle pole (magenta), in which sister *CEN3*s are not separated (green) or separated (blue) on the spindle. See Supplementary Note 4a and Supplementary Fig. S5 for information about *YFP–NIC96 KIP2–4GFP*.

data not shown). Thus, Ran GEF and +TIPs (Stu2, Bim1 and Bik1) are required to facilitate nuclear microtubule extension from spindle poles, and mutations to kinetochore components do not greatly affect this process. Ran GEF probably facilitates nuclear microtubule extension by increasing the nuclear concentration of RanGTP, because a Ran mutant also showed less frequent microtubule extension (data not shown). RanGTP may directly regulate microtubule dynamics in closed mitosis, as it does in open mitosis in *Xenopus* egg extracts[23,24]. At the very least, defects in nuclear microtubule extension in Ran GEF mutants were not secondary to

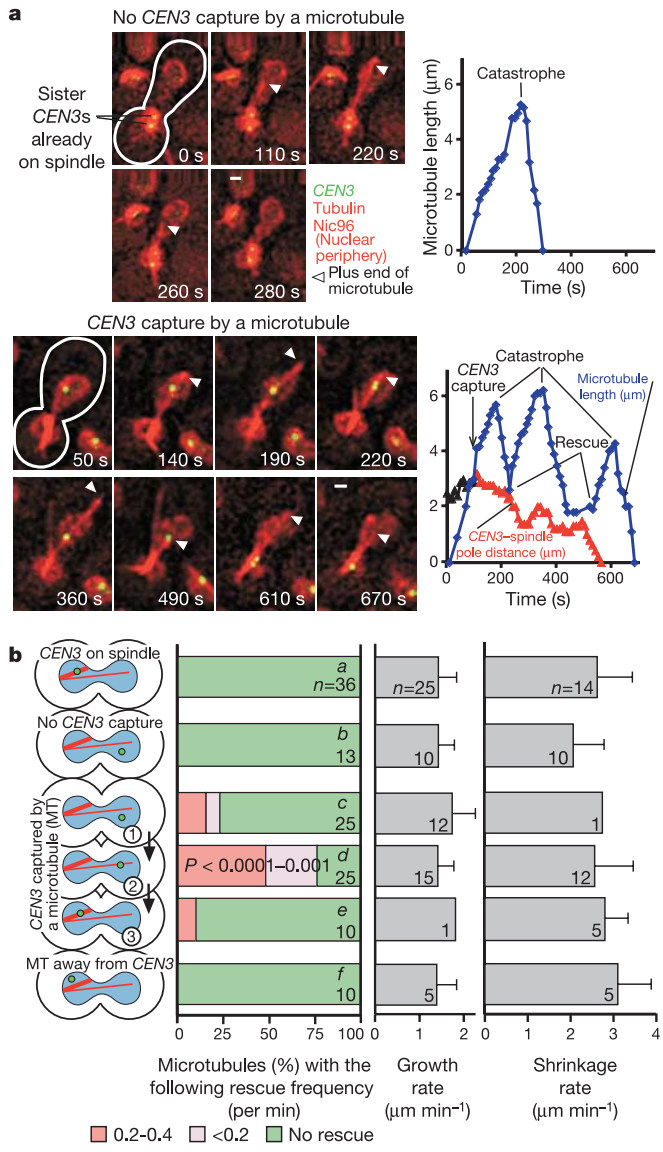

Figure 3 Captured kinetochores facilitate microtubule rescue. T3270 cells (see Fig. 2 legend) were treated as in Fig. 1c. **a**, Representative time-lapse images of nuclear microtubules that did not capture *CEN3* (top) and did capture *CEN3* (bottom). Scale bar, 1 μm. Graphs show microtubule length (blue). The lower graph also shows the distance of *CEN3* from a spindle pole before (black) and after (red) *CEN3* was captured by the microtubule. See Supplementary Videos S5 and S6. **b**, Dynamics of nuclear microtubules. Only microtubules that extended from the spindle towards the other side (towards the right in diagrams) of elongated nuclei were analysed, after cells were classified by *CEN3* location at the beginning of time-lapse and the fate of *CEN3* during observation. The rescue frequency of microtubules in bar *d* was significantly higher than that in *a*, *b*, *c* and *f* ($P < 0.0001$), and in *e* ($P < 0.001$). *n* represents the number of observed microtubules (left graph) or the number of observed events (middle and right graphs).

the nuclear import defects in these mutants. (See Supplementary Note 5.)

We then studied the kinetics of kinetochore capture by microtubules after *CEN3* reactivation in the above mutants. As expected, *CEN3* capture was delayed in yeast containing mutations to Ran GEF (Fig. 2c) and +TIPs (data not shown), where fewer nuclear microtubules extended. In *ndc10-1* (CBF3 complex), *spc24-1* and *spc25-1* (Ndc80 complex), *dsn1-7* and *mtw1-11* (Mtw1 complex), *okp1-5* (Ctf19 complex) and *rna1-1* (Ran GAP) mutants, the frequency of nuclear microtubule extension was comparable to wild-type cells, but a lack or significant delay in kinetochore capture was observed (Fig. 2c and data not shown). In contrast, *ipl1-321* and *sli15-3* mutants showed no significant delay in *CEN3* capture by microtubules. *spc34-3, ask1-3* and *dam1-1* (Dam1 complex) mutants also showed normal kinetics of *CEN3* capture, except for 10–15% of cells in which *CEN3* was not captured, perhaps owing to spindle abnormality (for example, spindle disruption). *ipl1-321, sli15-3, spc34-3, ask1-3* and *dam1-1* mutants showed no significant defects in *CEN3* transport along microtubules (data not shown). However, despite almost normal kinetics for *CEN3* capture and transport, these mutants showed a lack of or a severe delay in splitting the GFP signals of *CEN3* on the mitotic spindle after *CEN3* reached a spindle pole (Fig. 2c and data not shown).

Thus, the CBF3, Ndc80, Mtw1 and Ctf19 complexes, but not the Dam1 or Ipl1 complex, are necessary for kinetochore capture by the side of microtubules. In agreement with earlier reports[10,25–29], the Dam1 and Ipl1 complexes are required to ensure sister kinetochore bi-orientation. Ran GAP might facilitate kinetochore capture by microtubules, either by promoting nuclear import/export of unidentified regulators or by a more direct mechanism. (See Supplementary Note 6.)

Captured kinetochores facilitate microtubule rescue

After catastrophe (conversion from growth to shrinkage), nuclear microtubules shrank faster (2–3 μm min^{-1}) than the average velocity of poleward kinetochore transport (0.5–2.0 μm min^{-1}), whether or not the microtubules were associated with kinetochores (Fig. 3). One might therefore assume that the plus ends of shrinking microtubules would pass by the kinetochores, causing the kinetochores to slide off the microtubules. However, this never happened. To address the reason for it, we compared the dynamics of nuclear microtubules that did and did not capture *CEN3*. Microtubules did not show significant differences in growth rate or shrinkage rate while they were associated with *CEN3*. However, rescue (conversion from shrinkage to growth) was only observed for microtubules that were associated with *CEN3* at some stage, and not for other microtubules (Fig. 3 and Supplementary Videos S5 and S6). Owing to this microtubule rescue, the life span of microtubules that captured *CEN3* was significantly prolonged while they were associated with *CEN3* (Supplementary Fig. S7). Thus, kinetochores do not slide off microtubules because captured kinetochores facilitate microtubule rescue and extend microtubule life span. (See Supplementary Note 7.)

We next addressed whether *CEN3*-capturing microtubules are dynamic at their plus ends or at their minus ends (that is, at the ends distal or proximal to spindle poles, respectively). For this, we marked a region proximal to a spindle pole on 12 putative single microtubules by photobleaching the YFP–Tub1 signal (Fig. 4a and Supplementary Video S7). In all cases, while *CEN3*-associated microtubules shrank and grew, or while *CEN3* moved along the microtubules, there was no appreciable change in distance between the marked region and the spindle pole. Thus, microtubules shrink and grow mainly at their plus ends while they are associated with kinetochores. This property is reminiscent of cytoplasmic and anaphase nuclear microtubules in budding yeast[30]. The results also indicate that kinetochore transport is not due to microtubule flux towards a spindle pole[1].

Mechanisms of kinetochore-dependent microtubule rescue

How do kinetochores facilitate rescue of their associated microtubules? This rescue occurs preferentially when the microtubule plus ends come close to or reach the position of *CEN3* during microtubule shrinkage (Supplementary Fig. S8 and Supplementary Note 8). Nonetheless, microtubule rescue often happened even when *CEN3* was 1 μm or more away from the microtubule plus

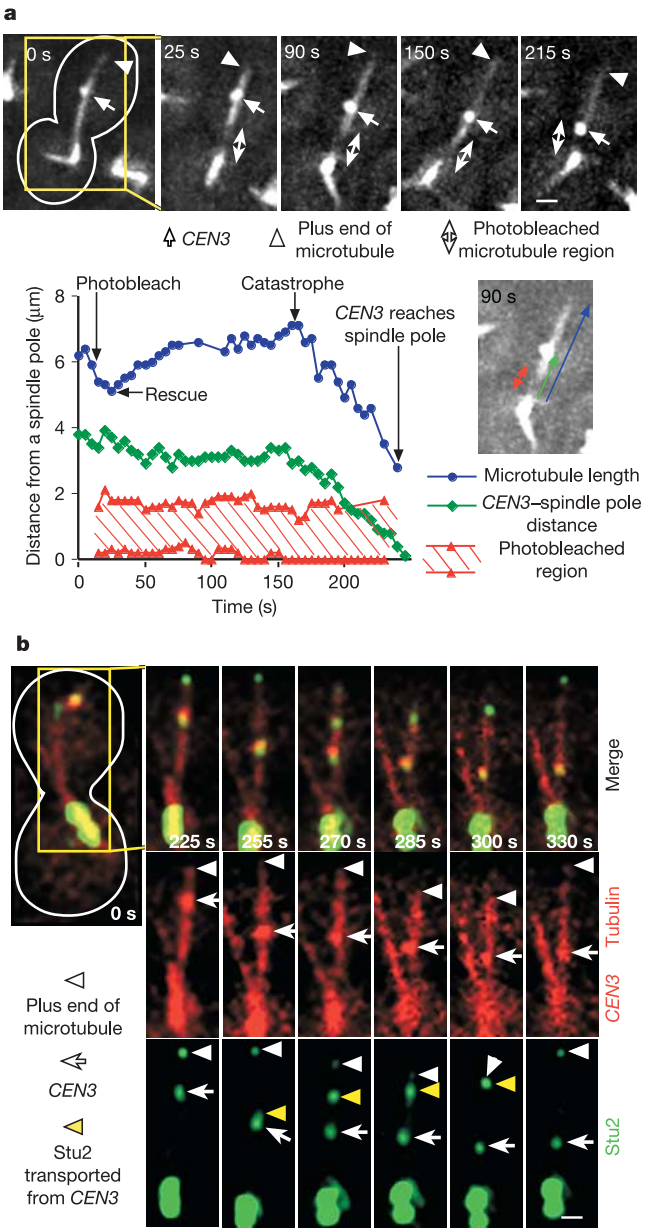

Figure 4 Microtubule rescue at the plus end coincides with the arrival of Stu2 protein transported from captured kinetochores. **a**, A kinetochore-associated microtubule shrinks and grows at its plus end. T3531 (see Fig. 1 legend) cells were treated as in Fig. 1c, except that GFP and YFP signals were collected together every 5 s. A microtubule region, proximal to a spindle pole, was photobleached between the 10 and 15 s time points while the microtubule was shrinking. See also Supplementary Video S7. **b**, Behaviour of Stu2 on a kinetochore-associated nuclear microtubule. *STU2–4GFP* P_{MET3}*-CDC20* P_{GAL}*-CEN3-tetOs TetR–3CFP CFP–TUB1* cells (T3680) were treated as in Fig. 1c, except that cyan fluorescent protein CFP (*CEN3* and tubulin, red) and GFP (Stu2, green) signals were collected separately every 15 s. Yellow arrowheads show Stu2–4GFP signals moving from *CEN3* to the microtubule plus end, along the microtubule. See also Supplementary Fig. S9. Scale bar (**a**, **b**) 1 μm.

end (Supplementary Fig. S8). The distribution of rescue positions can be explained, for instance, if kinetochores hold regulators that facilitate microtubule rescue, and if these regulators are occasionally translocated from captured kinetochores to the microtubule plus ends.

What could be the identity of such regulators? Stu2, Bim1 and Bik1 are good candidates, because they affect microtubule dynamics at the plus end[27,31–34] and facilitate the initial extension of nuclear microtubules (see above). Among the three candidates, only Stu2 (fused with 4 tandem copies of GFP) was detected on *CEN3* that had not yet been captured by microtubules (data not shown). Stu2 proteins localized to spindle poles and at the plus ends of extending nuclear microtubules (Fig. 4b). However, as microtubules reached their maximum length and subsequently shrank, Stu2 signals at the microtubule plus end gradually diminished (Fig. 4b, 225–285 s). Notably, after *CEN3* had been captured by the microtubule lattice, Stu2 was intermittently transported from *CEN3* along the microtubule towards the plus end (yellow arrowheads). The arrival of Stu2 at the microtubule plus end coincided with microtubule rescue (300–330 s). The transported Stu2 signal was not at the tip of another microtubule that might have overlapped with the existing longer microtubule (Supplementary Note 9b). We observed 24 rescues that occurred distal to *CEN3*, and all such rescues happened upon arrival of Stu2 (originating from *CEN3*) at the microtubule plus end (Supplementary Fig. S9). Arrival of Stu2 from *CEN3*, which occurred during microtubule shrinkage, almost always (in 24 out of 25 observations) led to immediate rescue (within 15 s) of the microtubule. Therefore, we propose that Stu2 is one of the mediators of kinetochore-dependent microtubule rescue. (See Supplementary Note 9.)

Kar3 kinesin is involved in kinetochore transport

What factors regulate kinetochore transport along the microtubule lattice? ATP-driven motor proteins could be involved. The *S. cerevisiae* genome encodes six kinesin family proteins (Cin8, Kar3, Kip1, Kip2, Kip3 and Smy1) and a single dynein heavy chain, Dyn1 (ref. 35). Among these motor proteins, Kar3 (a kinesin-14 family member) is thought to be the only nuclear microtubule minus-end directed motor. Kinetochore transport was studied in mutants containing single deletions of each these motor proteins. Except for *kar3* deletion, none of these mutations significantly altered kinetochore transport (data not shown). A *cin8-3 kip1Δ* double mutant[36] (Cin8 and Kip1 belong to the same kinesin-5 family) also had no delay in kinetochore transport (data not shown). In the majority of *kar3Δ* cells, *CEN3* was transported poleward as in wild-type cells (Fig. 5b). However, in a small number of *kar3Δ* cells, *CEN3* was at a 'standstill', staying longer (≥21 min) at almost the same position on microtubules, with no appreciable movement. We further examined the dominant-negative *kar3-1* mutant (known as a 'rigour' mutant) that can bind microtubules but does not have motor activity, owing to an ATP hydrolysis defect[37,38]. *kar3-1* cells showed longer and more frequent standstill than *KAR3*$^+$ cells (Fig. 5, Supplementary Fig. S10a and Supplementary Videos S8 and S9). Moreover, overexpression of Kar3 made *CEN3* move poleward along microtubules, with shorter pauses compared with control cells (*KAR3*$^+$) containing normal levels of Kar3 (Fig. 5, Supplementary Fig. S10b, Supplementary Videos S8 and S10). (See Supplementary Note 10.)

If Kar3 is involved in kinetochore transport, we would expect to find Kar3 loaded on kinetochores. Indeed, we found Kar3 association with centromeres using a chromatin immunoprecipitation assay. This association was (1) limited to a small centromeric region, (2) largely constant throughout the cell cycle, (3) dependent on Ndc10 and (4) probably independent of microtubule attachment to kinetochores (Supplementary Fig. S11 and Supplementary Note 11). In summary, Kar3 is involved in the poleward transport of kinetochores along microtubules. However, unidentified regulators probably act redundantly with Kar3, because kinetochore transport continued in the majority of cells with *kar3* deletions.

Capture of authentic centromeres in normal cell cycles

To address whether kinetochores on authentic centromeres associate with the microtubule lattice (without regulation by an adjacent *GAL1-10* promoter), we first studied the interaction of kinetochores (marked with Mtw1 and Ctf19, each fused with four tandem copies of GFP) with microtubules after cells were released from nocodazole arrest (Supplementary Fig. S12 and Supplementary Video S11).

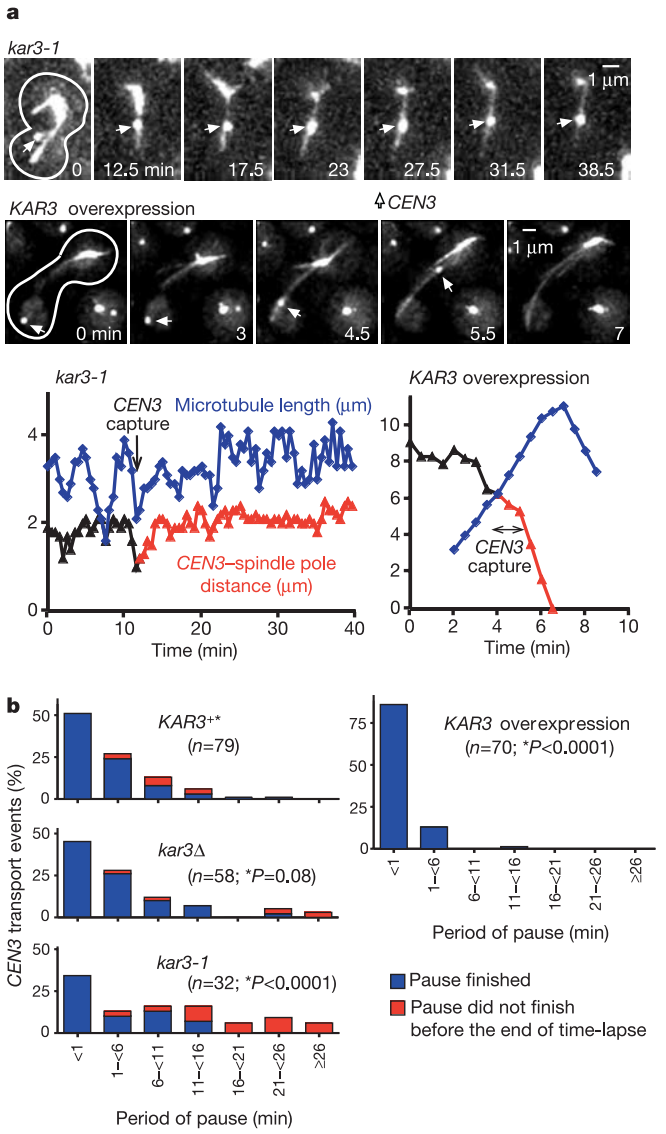

Figure 5 Kar3 kinesin is involved in the poleward transport of kinetochores along the side of microtubules. *KAR3*$^+$ cells (T3531, see Fig. 1 legend), cells with the same genotype but including *kar3Δ* (T2864) or *kar3-1* (T3319), and *PGAL-KAR3* cells (T3616) were treated as in Fig. 4a, except that time-lapse images were collected every 30 s for 40 min. **a**, *CEN3* pausing in a *kar3-1* cell (upper panel) and accelerated movement of *CEN3* in a cell overexpressing *KAR3* (lower panel). Scale bar, 1 μm. Graphs indicate microtubule length and *CEN3*–spindle pole distance in the two cells; colours as in Fig. 3a. See also Supplementary Fig. S10 and Supplementary Videos S8–10. **b**, Period of *CEN3* pause. Graphs show the percentage of *CEN3* transport events with the indicated pausing periods (the longest pause in each cell). Pauses that did not finish before the end of the time lapse (red) will have underestimated pause lengths. *n* refers to the number of observed *CEN3* transport events.

Soon after the microtubules had been reformed, several kinetochores moved along the microtubule lattice towards spindle poles.

Second, we released the above cells from α-factor arrest and tried to find individual kinetochore–microtubule interactions during S phase (determined by the emergence of small buds). Kinetochores on a single or a few chromosomes were sometimes found away from other kinetochores that clustered at a spindle pole (Fig. 6a and Supplementary Video S12). These isolated kinetochores seemed to be captured by the side of microtubules (Fig. 6a, 170 s) and transported poleward along microtubules (170–200 s). Such kinetochore association with the side of microtubules was not found in G1 or after establishment of the bipolar spindle.

Third, we used transmission electron microscopy (TEM) to observe nuclear microtubules and to locate centromeres. *CEN3, 4* and *5* were marked with adjacent *tet* operators bound by TetR–GFP in the same strain. The cells were frozen with high pressure during S phase, and processed for TEM and immuno-gold staining against GFP[39]. Clusters of two (or more) gold particles were found in the vicinity of microtubules only in cells with GFP-marked *CEN*s (that is, with both TetR–GFP and *tet* operators), but not in control cells (with TetR–GFP but without *tet* operators), suggesting that such clusters locate one of the GFP-marked centromeres. In some cells, the clusters were found in the vicinity of SPBs and associated with the side of microtubules (Fig. 6b). For instance, in the right panel of Fig. 6b, one of the *CEN*s seems to associate with a microtubule that extends from one of the duplicated but not-yet-separated SPBs (SPB2). Collectively, these results suggest that authentic centromeres associate laterally with microtubules during S phase of an unperturbed cell cycle. (See Supplementary Note 12.)

Discussion

We propose that the following steps occur during kinetochore capture by spindle microtubules in budding yeast (Fig. 6c and Supplementary Fig. S13). During the G1 phase of the cell cycle, kinetochores stay attached to microtubules and are localized in the vicinity of SPBs. Upon centromere DNA replication in early S phase, kinetochores are disassembled and centromeres detach from microtubules. Throughout much of S phase, assembly of a new SPB proceeds in the vicinity of an old SPB that is inherited from the previous cell cycle[9,40]. When kinetochores are reassembled on both replicated sister centromeres, more nuclear microtubules extend from the old SPB than from the new SPB that is not yet fully operational[10,11]. Microtubule extension is facilitated by +TIPs (Stu2, Bim1 and Bik1) and a high concentration of RanGTP in the nucleus, and it occurs in various directions (not only towards kinetochores). These microtubules (single microtubules in many cases) capture the kinetochores laterally. Capture requires the CBF3, Ndc80, Mtw1 and Ctf19 kinetochore complexes, but not the Ipl1 or Dam1 complex.

Once captured, kinetochores are transported along microtubules, predominantly towards spindle poles. The kinetochore-loaded Kar3 kinesin motor and other regulators drive this transport. Stu2 localizes at microtubule plus ends and at kinetochores that are not yet captured by microtubules. The amount of Stu2 protein at the microtubule plus end gradually decreases as microtubules shrink. However, after kinetochores have been captured, Stu2 protein is intermittently transported from kinetochores along microtubules towards their plus ends, where newly arrived Stu2 facilitates microtubule rescue (for example, Fig. 4b). In some cases, the plus ends of shrinking microtubules arrive at the kinetochores (for example, the first rescue in Fig. 3a, bottom) before Stu2 has been transported from kinetochores to microtubule plus ends. In such instances, microtubules are still rescued by Stu2, but this rescue occurs at the position of the kinetochore (the amount of Stu2 at the microtubule plus end increases upon rescue; data not shown). Without this rescue, kinetochores would frequently slide off microtubules, because microtubules shrink with a higher velocity than the

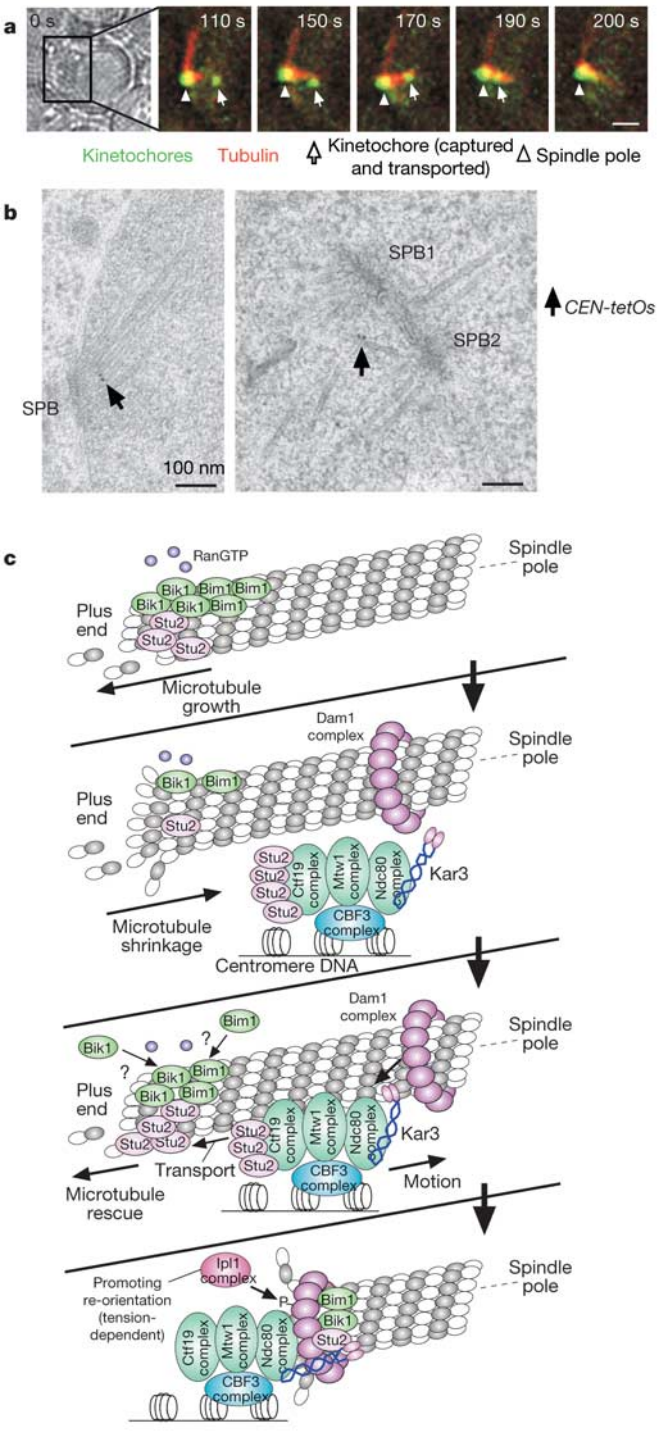

Figure 6 Association of authentic centromeres with microtubules in unperturbed cell cycles. **a**, *MTW1–4GFP CTF19–4GFP YFP–TUB1* cells (T3110) were treated with α-factor for 2.5 h and released to fresh medium. From 60 min after release, GFP and YFP images were acquired every 10 s. Scale bar, 1 μm. See also Supplementary Video S12. **b**, Transmission electron microscopy. *CEN3-tetOs CEN4-tetOs CEN5-tetOs TetR–GFP* cells (T2841) were fixed by high-pressure freezing when 50% showed bud emergence after release from α-factor arrest. Immuno-gold staining was against GFP. Arrows indicate clusters of two gold particles, marking the position of one of *CEN-tetOs*. Scale bar, 100 nm. **c**, Model for how microtubules interact with kinetochores, and which regulators are involved in kinetochore capture and transport along microtubules. Supplementary Fig. S13 shows a larger scale model.

average poleward motion of captured kinetochores. When kinetochores move along microtubules and approach a spindle pole, both sister kinetochores might attach to microtubules from the same pole (syntelic attachment)[10,11].

Later in S phase, the new SPB becomes functional and starts extending nuclear microtubules. Kinetochores change their associated microtubules from the old SPB to those of the new SPB, and continue to switch between the old and new SPBs. The Ipl1 kinase complex promotes this process through phosphorylation of kinetochore components (Dam1, Spc34 and possibly others)[10,41]. At the end of S phase, SPBs separate to form a bipolar spindle. As sister kinetochores bi-orient and each sister is pulled towards opposite spindle poles, tension is applied on kinetochore–spindle pole connections. When tension is applied, Ipl1-dependent re-orientation of kinetochore–spindle pole connections ceases, leading to stabilization of bi-orientation[18]. (See Supplementary Note 13.)

The Dam1 complex is required neither for kinetochore capture nor for transport along the microtubule lattice, but it is crucial for chromosome bi-orientation[26–29]. We propose that kinetochores use different contact molecules when they associate with microtubules laterally and when sister kinetochores bi-orient on the spindle (Fig. 6c). After kinetochore disassembly upon centromere DNA replication, the Ctf19, Mtw1 and Ndc80 complexes are probably assembled on replicated centromeres (dependent on the CBF3 complex[17,42–44]) before kinetochores first encounter microtubules, and one or more of the three complexes provides a direct interface with microtubules during lateral attachment to them. In contrast, the Dam1 complex on spindle microtubules is loaded on kinetochores (dependent on Ndc80) only after kinetochores are captured by microtubules[28,29] (see Supplementary Note 14). The Dam1 complex then acts to stabilize kinetochore–microtubule (perhaps end-on) attachments upon sister kinetochore bi-orientation[28]. The Dam1 complexes might facilitate kinetochore attachment at the plus end of a dynamic microtubule by forming a ring that encircles the microtubule[45,46].

In both vertebrate cells[2–4] and budding yeast, kinetochores are initially captured by microtubules on their lateral surface. Kinetochore attachment with the side of microtubules was also reported in diatoms[47]. This mechanism might have arisen early in the evolution of eukaryotic cells, because the microtubule lattice can secure initial kinetochore capture by providing a much larger contact surface for this capture compared with microtubule tips. However, to maintain association with kinetochores, the end-on attachment of microtubules might be more stable than the lateral attachment (see Supplementary Note 15). In fact, kinetochores sometimes detach from the microtubule lattice during their poleward transport.

Although kinetochores are captured by microtubules laterally in both budding yeast and vertebrate cells, we notice some important differences. First, microtubules extend from centrosomes preferentially in the direction of chromosomes in *Xenopus* egg extracts[48]. However, in budding yeast, microtubules do not preferentially extend in the direction of kinetochores. Because of the smaller size of its nucleus, yeast might not need such mechanisms. Second, kinetochores slide along the microtubule lattice much faster (11–14 $\mu m\,min^{-1}$ in newt lung cells[49]) in vertebrate cells than in budding yeast (0.5–2.0 $\mu m\,min^{-1}$). Whereas dynein is not involved in kinetochore transport along microtubules in *S. cerevisiae*, dynein might regulate fast kinetochore transport in vertebrate cells[2,50]. If this is the case, eukaryotic cells must have acquired the ability to use cytoplasmic dynein for kinetochore transport after they developed open mitosis. Alternatively, a member of the kinesin-14 family, to which Kar3 belongs, might be involved in fast kinetochore transport in vertebrate cells. (See Supplementary Note 16.)

Our study has revealed mechanisms for kinetochore capture by spindle microtubules in budding yeast. Kinetochore capture is the first crucial step for proper chromosome segregation in all eukaryotic cells. It is likely that, for such fundamental cellular events, some underlying mechanisms are conserved from yeast to vertebrates, even if modifications were added later in the evolutionary process. □

Methods

Yeast genetics and molecular biology

Yeast strain background (W303), methods for yeast culture, and the TetR–GFP/*tet* operator system were described previously[10,13,18]. Cells were cultured at 25 °C in YP medium containing glucose, unless otherwise stated. See Supplementary Note 17 for strain constructions, more culture conditions and mutant alleles used in this study.

Microscopy

The general procedures for time-lapse fluorescence microscopy were described previously[7]. Time-lapse images were collected every 10 s for 30 min at 23 °C (ambient temperature) unless otherwise stated. Using the Deltavision microscope (Applied Precision), we acquired 3–7 (0.7-μm apart) *z*-sections, which were subsequently deconvoluted and projected to two-dimensional images using SoftWoRx software (Applied Precision). Samples for TEM and immunostaining were prepared as previously described[39]. See Supplementary Note 18 for more details.

Analysing dynamics of nuclear microtubules

To analyse microtubule dynamics, we used time-lapse image sequences that were acquired every 10 s for 30 min, unless otherwise stated. To evaluate the length of microtubules and position of centromeres, we took account of the distance along the *z*-axis as well as distance on a projected image. Error bars in graphs show the 95% confidence interval (Fig. 2a, b) or the standard deviation (Figs 2c and 3b). See Supplementary Note 19 for more details.

Received 18 October 2004; accepted 18 February 2005; doi:10.1038/nature03483.

1. McIntosh, J. R., Grishchuk, E. L. & West, R. R. Chromosome-microtubule interactions during mitosis. *Annu. Rev. Cell Dev. Biol.* **18,** 193–219 (2002).
2. Rieder, C. L. & Alexander, S. P. Kinetochores are transported poleward along a single astral microtubule during chromosome attachment to the spindle in newt lung cells. *J. Cell Biol.* **110,** 81–95 (1990).
3. Hayden, J. H., Bowser, S. S. & Rieder, C. L. Kinetochores capture astral microtubules during chromosome attachment to the mitotic spindle: direct visualization in live newt lung cells. *J. Cell Biol.* **111,** 1039–1045 (1990).
4. Merdes, A. & De Mey, J. The mechanism of kinetochore-spindle attachment and polewards movement analyzed in PtK2 cells at the prophase-prometaphase transition. *Eur. J. Cell Biol.* **53,** 313–325 (1990).
5. Goshima, G. & Yanagida, M. Establishing biorientation occurs with precocious separation of the sister kinetochores, but not the arms, in the early spindle of budding yeast. *Cell* **100,** 619–633 (2000).
6. He, X., Asthana, S. & Sorger, P. K. Transient sister chromatid separation and elastic deformation of chromosomes during mitosis in budding yeast. *Cell* **101,** 763–775 (2000).
7. Tanaka, T., Fuchs, J., Loidl, J. & Nasmyth, K. Cohesin ensures bipolar attachment of microtubules to sister centromeres and resists their precocious separation. *Nature Cell Biol.* **2,** 492–499 (2000).
8. Pearson, C. G., Maddox, P. S., Salmon, E. D. & Bloom, K. Budding yeast chromosome structure and dynamics during mitosis. *J. Cell Biol.* **152,** 1255–1266 (2001).
9. Winey, M. & O'Toole, E. T. The spindle cycle in budding yeast. *Nature Cell Biol.* **3,** E23–E27 (2001).
10. Tanaka, T. U. *et al.* Evidence that the Ipl1-Sli15 (Aurora kinase-INCENP) complex promotes chromosome bi-orientation by altering kinetochore-spindle pole connections. *Cell* **108,** 317–329 (2002).
11. Tanaka, T. U. Chromosome bi-orientation on the mitotic spindle. *Phil. Trans. R. Soc. Lond. B* (in the press); doi:10.1098/rstb.2004.1612.
12. Hill, A. & Bloom, K. Genetic manipulation of centromere function. *Mol. Cell. Biol.* **7,** 2397–2405 (1987).
13. Michaelis, C., Ciosk, R. & Nasmyth, K. Cohesins: chromosomal proteins that prevent premature separation of sister chromatids. *Cell* **91,** 35–45 (1997).
14. Nasmyth, K., Peters, J. M. & Uhlmann, F. Splitting the chromosome: cutting the ties that bind sister chromatids. *Science* **288,** 1379–1385 (2000).
15. O'Toole, E. T., Winey, M. & McIntosh, J. R. High-voltage electron tomography of spindle pole bodies and early mitotic spindles in the yeast *Saccharomyces cerevisiae*. *Mol. Biol. Cell* **10,** 2017–2031 (1999).
16. Gupta, M. L. Jr *et al.* β-Tubulin C354 mutations that severely decrease microtubule dynamics do not prevent nuclear migration in yeast. *Mol. Biol. Cell* **13,** 2919–2932 (2002).
17. McAinsh, A. D., Tytell, J. D. & Sorger, P. K. Structure, function, and regulation of budding yeast kinetochores. *Annu. Rev. Cell Dev. Biol.* **19,** 519–539 (2003).
18. Dewar, H., Tanaka, K., Nasmyth, K. & Tanaka, T. U. Tension between two kinetochores suffices for their bi-orientation on the mitotic spindle. *Nature* **428,** 93–97 (2004).
19. Akhmanova, A. & Hoogenraad, C. C. Microtubule plus-end-tracking proteins: mechanisms and functions. *Curr. Opin. Cell Biol.* **17,** 47–54 (2005).
20. Corbett, A. H. & Silver, P. A. Nucleocytoplasmic transport of macromolecules. *Microbiol. Mol. Biol. Rev.* **61,** 193–211 (1997).
21. Hetzer, M., Gruss, O. J. & Mattaj, I. W. The Ran GTPase as a marker of chromosome position in spindle formation and nuclear envelope assembly. *Nature Cell Biol.* **4,** E177–E184 (2002).
22. Quimby, B. B. & Dasso, M. The small GTPase Ran: interpreting the signs. *Curr. Opin. Cell Biol.* **15,** 338–344 (2003).
23. Wilde, A. *et al.* Ran stimulates spindle assembly by altering microtubule dynamics and the balance of motor activities. *Nature Cell Biol.* **3,** 221–227 (2001).
24. Carazo-Salas, R. E., Gruss, O. J., Mattaj, I. W. & Karsenti, E. Ran-GTP coordinates regulation of microtubule nucleation and dynamics during mitotic-spindle assembly. *Nature Cell Biol.* **3,** 228–234 (2001).
25. Biggins, S. *et al.* The conserved protein kinase Ipl1 regulates microtubule binding to kinetochores in budding yeast. *Genes Dev.* **13,** 532–544 (1999).
26. Cheeseman, I. M., Enquist-Newman, M., Muller-Reichert, T., Drubin, D. G. & Barnes, G. Mitotic

spindle integrity and kinetochore function linked by the Duo1p/Dam1p complex. *J. Cell Biol.* **152,** 197–212 (2001).
27. He, X., Rines, D. R., Espelin, C. W. & Sorger, P. K. Molecular analysis of kinetochore-microtubule attachment in budding yeast. *Cell* **106,** 195–206 (2001).
28. Janke, C., Ortiz, J., Tanaka, T. U., Lechner, J. & Schiebel, E. Four new subunits of the Dam1–Duo1 complex reveal novel functions in sister kinetochore biorientation. *EMBO J.* **21,** 181–193 (2002).
29. Li, Y. *et al.* The mitotic spindle is required for loading of the DASH complex onto the kinetochore. *Genes Dev.* **16,** 183–197 (2002).
30. Maddox, P. S., Bloom, K. S. & Salmon, E. D. The polarity and dynamics of microtubule assembly in the budding yeast *Saccharomyces cerevisiae*. *Nature Cell Biol.* **2,** 36–41 (2000).
31. Tirnauer, J. S., O'Toole, E., Berrueta, L., Bierer, B. E. & Pellman, D. Yeast Bim1p promotes the G1-specific dynamics of microtubules. *J. Cell Biol.* **145,** 993–1007 (1999).
32. van Breugel, M., Drechsel, D. & Hyman, A. Stu2p, the budding yeast member of the conserved Dis1/XMAP215 family of microtubule-associated proteins is a plus end-binding microtubule destabilizer. *J. Cell Biol.* **161,** 359–369 (2003).
33. Lin, H. *et al.* Polyploids require Bik1 for kinetochore–microtubule attachment. *J. Cell Biol.* **155,** 1173–1184 (2001).
34. Carvalho, P., Gupta, M. L. Jr, Hoyt, M. A. & Pellman, D. Cell cycle control of kinesin-mediated transport of Bik1 (CLIP-170) regulates microtubule stability and dynein activation. *Dev. Cell* **6,** 815–829 (2004).
35. Hildebrandt, E. R. & Hoyt, M. A. Mitotic motors in *Saccharomyces cerevisiae*. *Biochim. Biophys. Acta* **1496,** 99–116 (2000).
36. Saunders, W. S., Koshland, D., Eshel, D., Gibbons, I. R. & Hoyt, M. A. *Saccharomyces cerevisiae* kinesin- and dynein-related proteins required for anaphase chromosome segregation. *J. Cell Biol.* **128,** 617–624 (1995).
37. Meluh, P. B. & Rose, M. D. *KAR3*, a kinesin-related gene required for yeast nuclear fusion. *Cell* **60,** 1029–1041 (1990).
38. Maddox, P. S., Stemple, J. K., Satterwhite, L., Salmon, E. D. & Bloom, K. The minus end-directed motor Kar3 is required for coupling dynamic microtubule plus ends to the cortical shmoo tip in budding yeast. *Curr. Biol.* **13,** 1423–1428 (2003).
39. Muller-Reichert, T. *et al.* Analysis of the distribution of the kinetochore protein Ndc10p in *Saccharomyces cerevisiae* using 3-D modeling of mitotic spindles. *Chromosoma* **111,** 417–428 (2003).
40. Adams, I. R. & Kilmartin, J. V. Spindle pole body duplication: a model for centrosome duplication? *Trends Cell Biol.* **10,** 329–335 (2000).
41. Cheeseman, I. M. *et al.* Phospho-regulation of kinetochore-microtubule attachments by the Aurora kinase Ipl1p. *Cell* **111,** 163–172 (2002).
42. Westermann, S. *et al.* Architecture of the budding yeast kinetochore reveals a conserved molecular core. *J. Cell Biol.* **163,** 215–222 (2003).
43. Nekrasov, V. S., Smith, M. A., Peak-Chew, S. & Kilmartin, J. V. Interactions between centromere complexes in *Saccharomyces cerevisiae*. *Mol. Biol. Cell* **14,** 4931–4946 (2003).
44. De Wulf, P., McAinsh, A. D. & Sorger, P. K. Hierarchical assembly of the budding yeast kinetochore from multiple subcomplexes. *Genes Dev.* **17,** 2902–2921 (2003).
45. Miranda, J. L., De Wulf, P., Sorger, P. & Harrison, S. C. The yeast DASH complex forms closed rings on microtubules. *Nature Struct. Mol. Biol.* **12,** 138–143 (2005).
46. Westermann, S. *et al.* Formation of a dynamic kinetochore-microtubule interface through assembly of the Dam1 ring complex. *Mol. Cell* **17,** 277–290 (2005).
47. Pickett-Heaps, J. D. Cell division in diatoms. *Int. Rev. Cytol.* **128,** 63–107 (1991).
48. Carazo-Salas, R. E. & Karsenti, E. Long-range communication between chromatin and microtubules in *Xenopus* egg extracts. *Curr. Biol.* **13,** 1728–1733 (2003).
49. Alexander, S. P. & Rieder, C. L. Chromosome motion during attachment to the vertebrate spindle: initial saltatory-like behavior of chromosomes and quantitative analysis of force production by nascent kinetochore fibers. *J. Cell Biol.* **113,** 805–815 (1991).
50. King, J. M., Hays, T. S. & Nicklas, R. B. Dynein is a transient kinetochore component whose binding is regulated by microtubule attachment, not tension. *J. Cell Biol.* **151,** 739–748 (2000).

Supplementary Information accompanies the paper on **www.nature.com/nature**.

Acknowledgements We thank J. R. Swedlow, M. J. R. Stark, A. Gartner, M. A. Hoyt, A. Desai, P. R. Clarke, P. D. Andrews and members of the Tanaka laboratory for discussions and for reading the manuscript; T. Hyman, K. Nasmyth, I. W. Mattaj, E. Karsenti, F. Uhlmann and J. Ellenberg for discussions; J.-F. Maure, N. Rachidi and M. J. R. Stark for sharing their unpublished data; Y. Kitamura, S. Swift, M. Romao and G. Keir for technical help; F. Wheatley and the media kitchen for media preparation; M. A. Hoyt, D. Pellman, R. Ciosk, F. Uhlmann, K. Nasmyth, T. C. Huffaker, J. V. Kilmartin, E. Schiebel, S. Biggins, C. S. M. Chan, I. M. Cheeseman, G. Barnes, R. Tsien, S. J. Elledge, J. Lechner, A. H. Corbett, P. A. Silver, P. K. Sorger, X. He, A. F. Straight, M. D. Rose, V. Doye, F. Severin, I. Ouspenski, K. Bloom, T. Nishimoto, J. E. Haber, T. N. Davis, EUROSCARF and the Yeast Resource Center for reagents. This work was supported by The Wellcome Trust, Cancer Research UK and the EMBO Young Investigator Program.

Competing interests statement The authors declare that they have no competing financial interests.

Correspondence and requests for materials should be addressed to T.U.T (t.tanaka@dundee.ac.uk).